Highly localized thermal, mechanical, and spectroscopic characterization of polymers using miniaturized thermal probes

A. Hammiche,[a] L. Bozec, M. Conroy, and H. M. Pollock
Department of Physics, Lancaster University, Lancaster LA1 4YB, United Kingdom

G. Mills and J. M. R. Weaver
Department of Electronics and Electrical Engineering, University of Glasgow, Glasgow GI2 8LT, United Kingdom

D. M. Price, M. Reading, D. J. Hourston, and M. Song
IPTME, Loughborough University, Loughborough LE11 3TU, United Kingdom

(Received 9 September 1999; accepted 10 March 2000)

In this article, we demonstrate the versatility of use of cantilever-type resistive thermal probes. The probes used are of two kinds, Wollaston wire probes and batch-microfabricated probes. Both types of probe can be operated in two modes: a passive mode of operation whereby the probe acts as a temperature sensor, and an active mode whereby the probe acts also as a highly localized heat source. We present data that demonstrate the characterization of some composite polymeric samples. In particular, the combination of scanning thermal microscopy with localized thermomechanometry (or localized thermomechanical analysis, L-TMA) shows promise. Comparison with data from conventional bulk differential scanning calorimetry shows that inhomogeneities within materials that cannot be detected using conventional bulk thermal methods are revealed by L-TMA. We also describe a new mode of thermal imaging, scanning thermal expansion microscopy. Finally, we outline progress towards the development of localized Fourier transform infrared spectroscopy: here the probe, in this case operated in the temperature-sensing mode, detects the photothermal response of a specimen exposed to the beam and heated thereby. [S0734-211X(00)11303-4]

I. INTRODUCTION

A number of analytical techniques that operate on bulk samples to obtain macroscopic information may, in principle, be combined with scanning probe microscopy. The combination of localized thermal analysis with near-field microscopy has been termed micro-thermal analysis.[1,2] The parent technique is that of scanning thermal microscopy (SThM), in which an ''active'' thermal probe is also used as a heater, so as to inject critically damped temperature waves into a sample and to allow subsurface imaging of polymers and other materials.[3–6] The subsurface detail detected corresponds to variations in heat capacity or thermal conductivity. Localized thermal analysis (L-TA) builds upon this technique, in order to add spatial discrimination to three well-established methods of chemical fingerprinting, namely thermomechanometry, calorimetry, and spectroscopy.

In thermal analysis, a temperature ramp is used to reveal physical events in the sample such as a glass transition or melting. For example, in modulated-temperature differential scanning calorimetry, a cyclic heat flow signal ''sees'' only the reversible heat capacity. This is associated with molecular vibrations during all transitions except melting, in which case this cyclic signal may also include a contribution from the melting of crystallites having a distribution of melting temperatures. The underlying measurement, equivalent to a conventional differential scanning calorimetry experiment, also detects endotherms and exotherms associated with kinetically controlled processes. In dynamic thermomechanical analysis, the thermal transitions are revealed through changes in the real and imaginary parts of the elastic modulus. In L-TA, the chief advantages of using the active thermal probe to provide the temperature ramp as well as the modulation, without the use of a heating stage, are: (a) the data are obtained from localized regions chosen from a previously obtained thermal image, (b) apart from these regions, the rest of the sample is preserved in its original unheated state, avoiding the risk that it will be irreversibly altered (in which case it will be impossible to achieve the usual objective of microscopical examination, namely the characterization of a material in its as-received state).

We are developing these new techniques for performing localized nondestructive analysis on individual regions of a solid sample, selected by means of scanning probe microscopy at micrometer spatial resolution. Our chief interest has been in probing the thermomechanical and optical properties of polymeric systems. Micro-thermal analysis is now being used commercially to characterize materials and surfaces, visualizing the spatial distribution of phases, components, and contaminants in substances such as polymers, pharmaceuticals, and foods.[5–7] We describe here the following:

(1) the combination of SThM with localized thermomechanometry (or localized thermomechanical analysis, L-TMA),

[a]Electronic mail: a.hammiche@lancaster.ac.uk

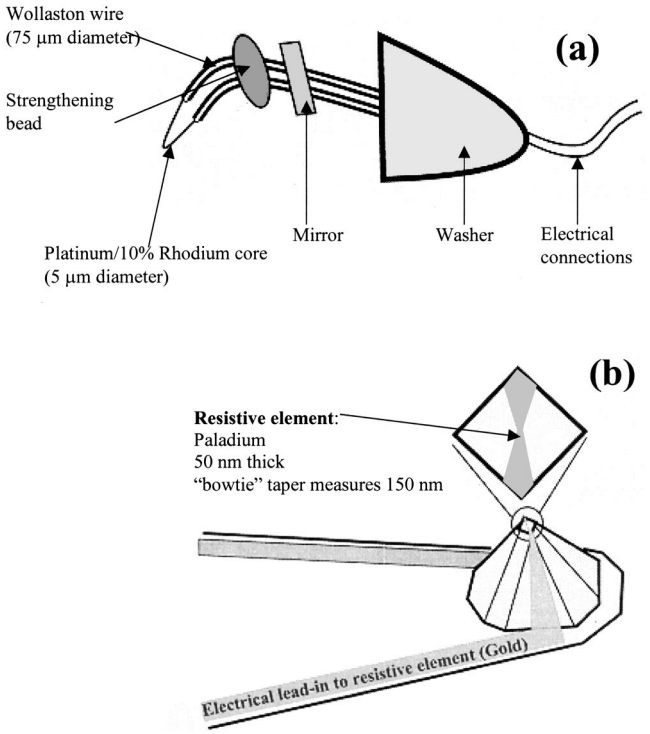

FIG. 1. Schematic diagram of the Wollaston wire (a) and the micromachined (b) probes.

(2) a comparison of data obtained by L-TMA and by conventional bulk thermal analysis, in this case differential scanning calorimetry (DSC),
(3) scanning thermal expansion microscopy as a new mode of thermal imaging,
(4) an outline of recently published progress towards the development of localized Fourier transform infrared (FTIR) spectroscopy,[8] including recent results: here the probe, in this case operated in the temperature-sensing mode, detects the photothermal response of a specimen exposed to the beam and heated thereby.

II. INSTRUMENTATION

We use two types of probe (Fig. 1) that allow for force feedback as well as thermal feedback, and thus serve as both atomic force microscopy (AFM) and thermal probes. In each case, the probe performs three functions: it exerts a force on the sample surface; it is a source of heat, either constant or modulated; and it measures heat flow. As described elsewhere,[2,3] probes can be used in either of two operating modes:

(1) a temperature sensing mode: a small constant current is passed through the probe. The probe temperature is then monitored by measuring the voltage across it;
(2) a heating mode: the probe is then self-heating when a large current is passed through it. The thermal element of the probe then acts as a highly localized heat source. A temperature rise of up to a few hundred degrees can be achieved. The temperature of this heat source can be maintained constant, modulated and/or ramped. Because of the small size of the probe and of the region of sample being heated at any one time, heating and cooling may be very rapid, the rate of data acquisition is high, and temperature modulation frequencies in the tens of kilohertz range may be used.

The Wollaston wire probes used [Fig. 1(a)], as well as the AFM system (''Explorer'' model), were supplied by ThermoMicroscopes (TopoMetrix Corporation). As described elsewhere,[1,3] the sensing element is a 5-μm-diam platinum/10% rhodium wire of length $\sim$200 μm, and the measured spring constant is $\sim$10 N/m. The micromachined probes [Fig. 1(b)] are fabricated at Glasgow University Nanoelectronics Research Centre. They are produced in batches of 240 and 60 (full or $\frac{1}{4}$ wafer) using photolithography, potassium hydroxide etching and multiple-level electron beam lithography.[9] The resistive element is formed by patterning an abrupt taper in a palladium wire that runs across the flattened apex (2.5×2.5 μm square) of the 20-μm-high pyramid. This produces a localized high resistance, which varies between 250 and 1000 Ω depending on what dimensions are chosen for the palladium wire. Taper widths of 150 nm are commonplace. Electrical lead-ins to the resistive element are patterned along the cantilever and up the sides of the pyramid. The measured spring constant is $\sim$0.2 N/m.

III. POLYMERS CHARACTERIZED USING THE COMBINATION OF SThM WITH LOCALIZED THERMOMECHANOMETRY (OR LOCALIZED THERMOMECHANICAL ANALYSIS, L-TMA)

In SThM, the probe is raster scanned across the surface of the sample in force feedback mode allowing topography to be recorded. In addition, the temperature of the heating element is maintained constant by forcing its resistance to be kept constant through a feedback mechanism. This thermal feedback signal is used to construct an image whose contrast represents variation in the amount of heat flowing out of the probe. This is determined to a large extent by the variations in thermal conductivity at the surface and near surface.

Once an area has been scanned and images acquired, the probe is moved to selected locations on the surface and thermomechanical measurements are performed at these locations. This is achieved by pressing the probe tip against the sample, leading to a deflection of the cantilever, with a given starting force, and with force feedback disengaged. The temperature at the contact point is then ramped up and down. If the material undergoes a phase transition, its mechanical properties vary, leading to a change in the interaction force and thus a change in the deflection of the cantilever. Hence, monitoring of the cantilever deflection permits the detection of phase transitions. Because of the small size of the heating element and the small amount of material involved, heating and cooling may be very rapid. The thermal time constant involved is estimated at a few microseconds. The fastest ramp rate that is presently achieved is 1400 °C/min. This limit is set by the computer processing time involved when setting the temperature, digitizing and reading in the data.

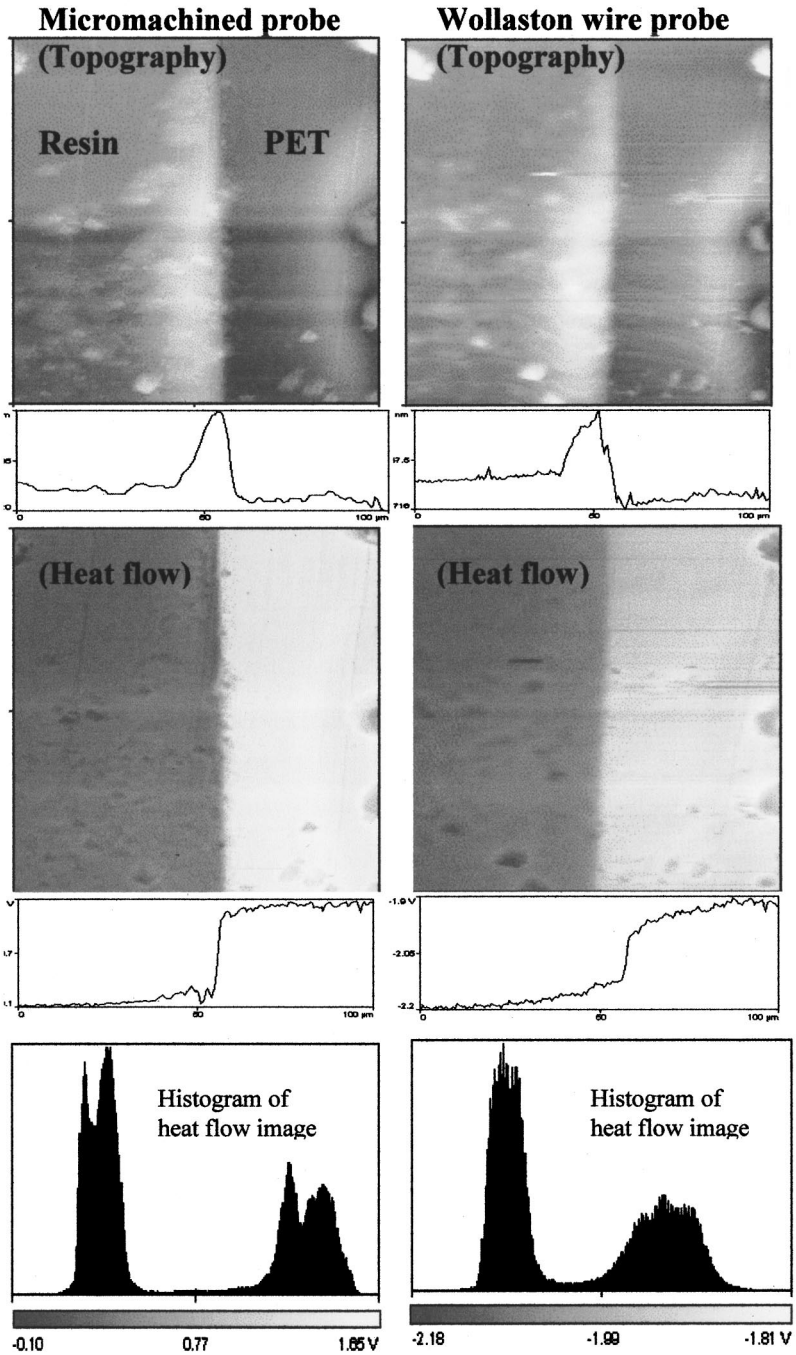

FIG. 2. Topography and heat flow images of a polyethylene terephthalate (PET)/acrylic resin composite polymeric sample recorded using Wollaston wire and micromachined probes.

To demonstrate the principle, we use a composite polymeric sample made from a 0.5-mm-thick film of polyethylene terephthalate (PET) immersed in a hydrophilic acrylic resin. The resin was cured by heating at 60 °C for 24 h. The sample was then microtomed to achieve as flat a surface as possible, revealing the embedded PET. This model sample is used in order to minimize the effects of subsurface variations in thermal properties and the effects of topography upon the thermal signal. First, the same area of the sample was scanned with both probes at a constant temperature (about 30 °C above room temperature) and a constant force. Both topography and heat flow images were recorded.

Figure 2 shows topography and heat flow images obtained when scanning across the PET/resin boundary. The PET region shows brighter in the heat flow images indicating a higher apparent thermal conductivity. The boundary is sharper in the heat flow images. Probe-sample contact area can vary, due to the convolution of the probe shape with the residual topography of the sample, and this can lead to purely topographical features being observed in the heat flow images. As expected, the heat flow images recorded using the micromachined probe are sharper, and this observation is further confirmed when considering histograms and scan lines. The two main peaks in the histograms corresponding to the higher and lower thermal conductivities are more neatly separated in the image taken with the micromachined

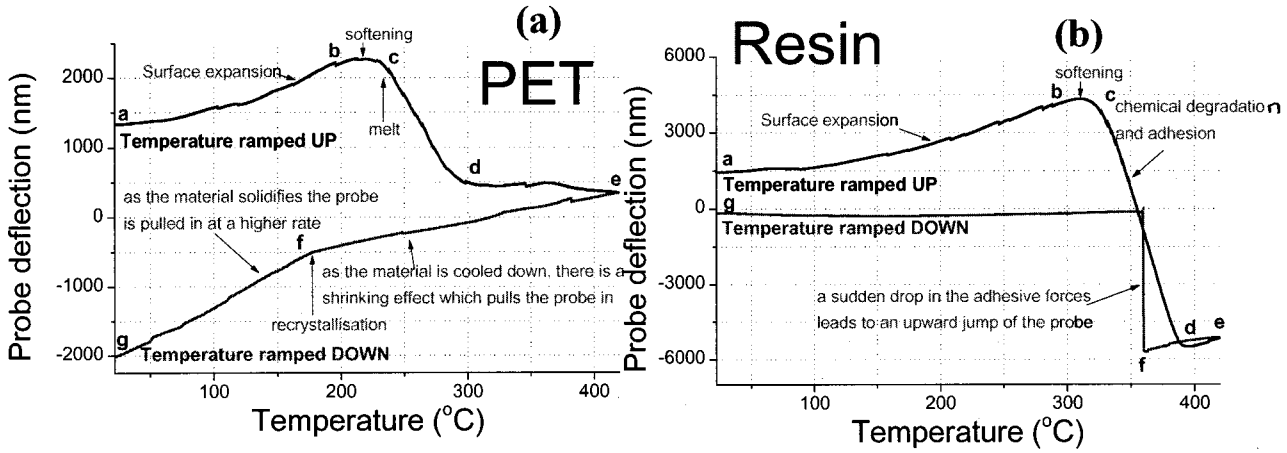

FIG. 3. Localized thermomechanical analysis traces recorded with a Wollaston wire thermal probe on the PET/resin composite sample. Measurements are performed with a starting pressing force of 10 μN and a temperature ramp rate of 8 °C/s.

probe. A sharper transition from one region to the next is also observed in the heat flow scan lines. It should be noted that with this very low-topography sample, in the topographic images there is little difference in the resolution of the boundary given by the two types of probe: quantitative evidence for the improvement in spatial resolution given by the micromachined probes, when imaging different types of sample, will be presented in a future publication.

Further information is then obtained by performing L-TMA at both regions. The results obtained, using a Wollaston wire probe, are shown in Figs. 3 and 4. A 10 μN starting force was used for both measurements. The traces are divided into a number of segments. Figure 3(a) shows the underlying Wollaston wire probe deflection as temperature is ramped at a rate of 8 °C/s on the PET part of the sample, up to 420 °C and then back to room temperature. As the material under the probe is heated it expands, deflecting the probe upward (ab); the PET then softens leading to plastic deformation under the pressing probe (bc); the PET then melts (at between 230 and 260 °C as confirmed by conventional DSC) and the tip of the probe sinks into the material (cd) and (de); on cooling, material further away from the surface solidifies and shrinks leading to capillary forces within the still molten material to pull the probe further in (ef); as material closer to the tip then solidifies further shrinking occurs, and the probe is pulled in at a higher rate (fg). Figure 3(b) shows plots resulting from a similar measurement on the resin part of the sample. Surface expansion is first observed (ab), then softening and chemical degradation (a conventional DSC measurement confirmed that there was no phase transition), leading to an increased probe/sample contact area. The resulting increased adhesion then pulls the tip into the sample as a decrease in volume of material takes place (bc); on cooling further shrinking of the material pulls the probe further in up to point d, so that the deflected cantilever is exerting an increasing negative (tensile) force. When this reaches a critical ''pull off'' value, the adhesion can no longer maintain the contact and the probe is then released away from the surface (d'e). Figure 4(a) illustrates the relative strengths of the forces experienced by the probe on the PET and the resin. Figure 4(b) shows the differential of the laser deflection to illustrate the relative temperatures at which the thermal

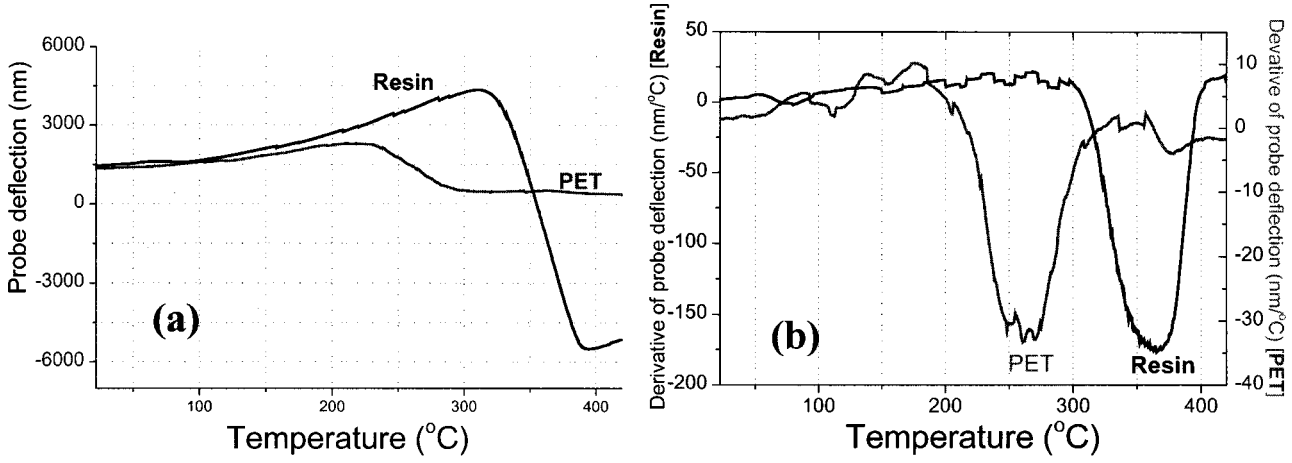

FIG. 4. Plots of probe deflection (a) and first derivative of probe deflection (b) recorded when the temperature is ramped up comparing local surface deformations in the two materials (a) and temperatures at which the main thermal events take place (b).

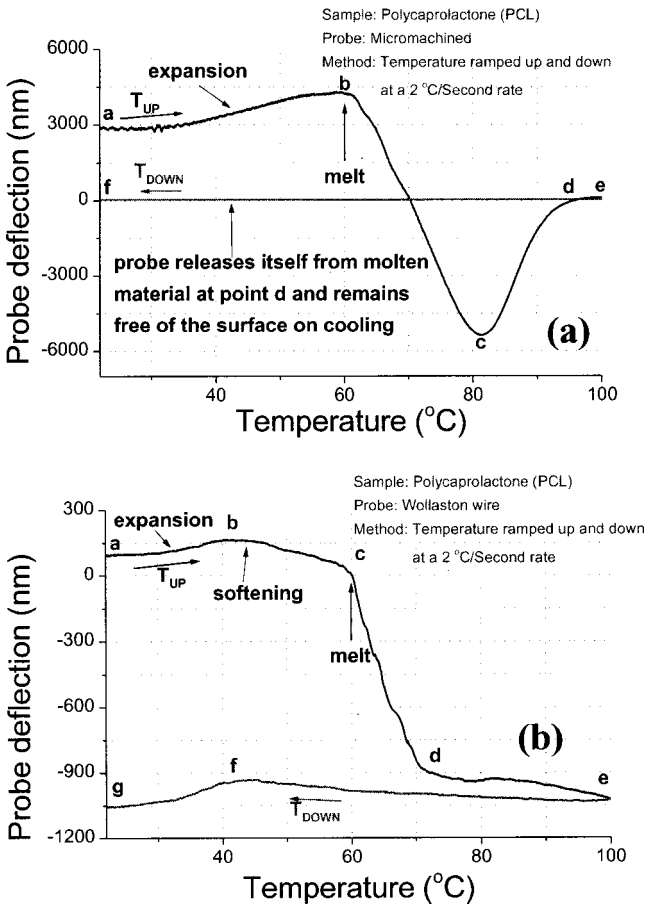

FIG. 5. Localized thermomechanical plots of a polycaprolactone (PCL) sample recorded using a micromachined probe (a) and a Wollaston wire probe.

events (melt for PET and chemical degradation for the resin) take place.

Either type of thermal probe may be used to obtain L-TMA data. This is shown by the data summarized in Fig. 5, where the sample used was polycaprolactone (PCL). Graphs of probe deflection versus temperature show that the melting point (60 °C) is clearly detected as the temperature is ramped up. The material first expands, then melting occurs, resulting in the probe sinking into the sample. Negative forces exerted by the molten material pull the probe in beyond its zero deflection setting. In the case of the micromachined probe, these forces are less effective above about 80 °C (point c), and the probe gradually releases itself from the material. On cooling recrystallization is not detected. The measurement with the Wollaston probe reveals a transition at about 45 °C, which could be a glass transition. This is not a probe-dependent effect: rather, it indicates that at that particular location the volume of material heated is not fully crystalline. On cooling, the transition at 45 °C is detected. Full interpretation of such curves has to take into account the mechanical properties of the probes (in particular the spring constant) and the fact that the temperature profile is continuously changing within the heated volume. Different phase transitions involving different parts of the material lead to competing effects on the probe deflection.

Clearly when the active mode of thermal imaging is used, interpretation of image contrast must take into account a number of parameters including:

(1) the effective contact area between probe and sample surface topography,
(2) contaminants on the surface,
(3) possible heating effects due to friction during scanning.

Since a temperature gradient exists which extends below the surface, subsurface structures within the thermal gradient will affect heat flow and thus image contrast. When used to perform thermomechanical analysis, full interpretation of traces obtained requires knowledge of the mechanical properties of the probe, in particular its spring constant. This we intend to achieve by mathematical analysis and modeling.

IV. COMPARISON BETWEEN DATA OBTAINED BY L-TMA AND BY CONVENTIONAL BULK THERMAL ANALYSIS (DSC)

We have analyzed samples of commercial grade quenched polyethylene terephthalate (PET) using (a) the localized thermomechanical method, and (b) a conventional bulk thermal method, namely DSC). The samples are in the form of pellets a few mm^3 in volume. The aim is to compare the two methods in terms of the information obtained and show that inhomogeneities within materials that cannot be detected using conventional bulk thermal methods are revealed by localized thermomechanical analysis.

Figure 6 shows plots of heat flow versus temperature obtained from DSC measurements. Heating and cooling were performed at 10 °C/min. The first analysis of the material as supplied [Fig. 6(a)] shows a glass transition at 75 °C, a recrystallization at 130 °C, and a melt at 260 °C upon heating. As the sample is cooled, a recrystallization is observed at 180 °C. Figure 6(b) shows DSC traces of the same sample upon a second heating. The glass transition is now much smaller, and no recrystallization takes place on heating.

These differences are due to the thermal history of the material. The sample that is supplied has been cooled before it has had time to fully crystallize after processing; consequently, there are large amorphous regions, which give rise to a large glass transition signal. As the sample is heated above the glass transition temperature, the sample has enough energy and flexibility to crystallize to a significant degree: hence the recrystallization peak in the heating cycle. The slow cooling in the DSC gives the PET enough time to crystallize before it is below its glass transition temperature. The slow cooling leads to more recrystallization, so that the glass transition signal is much smaller and there is no recrystallization upon heating [Fig. 6(b)].

The samples were then analyzed with the Wollaston wire probe. All measurements were done at a 70 °C/min heating and cooling rate. The analysis of the surface of a PET pellet shows no evidence of a glass transition [Fig. 7(a)], indicating that the surface is highly crystalline. On heating, a linear

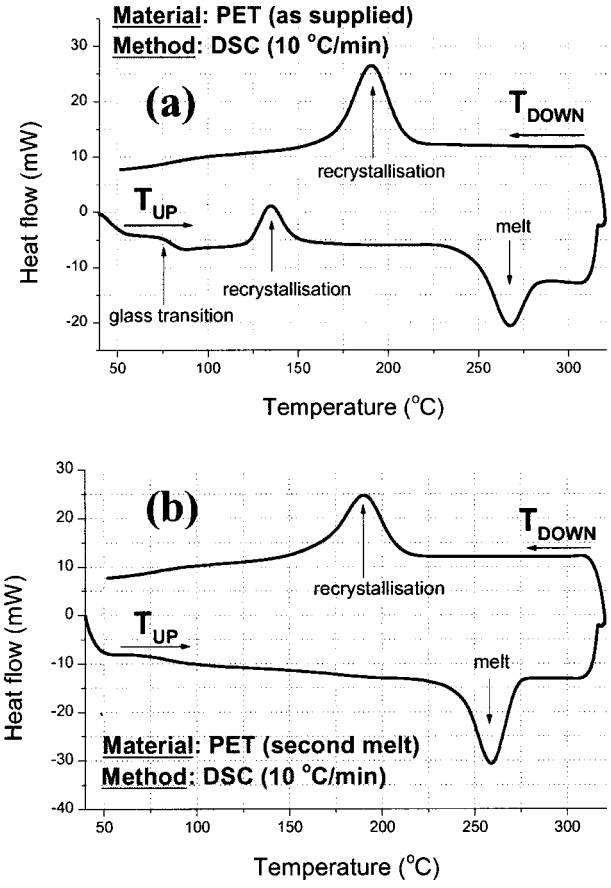

FIG. 6. Conventional differential scanning calorimetry (DSC) plots of quenched polyethylene terephthalate, (a) results of analysis of a sample of material as supplied (first melt) and (b) result after the same sample is analyzed a second time (second melt).

surface expansion up to the melting point (segment ab) is observed. Then as material melts, the probe breaks through the surface and penetrates the material up to a certain depth (segment bc) where it remains roughly at the same level (segment cd). On cooling, the material contracts, pulling the probe further in (segment de).

The pellet was then cut in half and the cut face was analyzed. A glass transition, a recrystallization and a melt are all identified in the heating cycle [Fig. 7(b)]. On heating, as the material undergoes a glass transition, it softens and deforms under the pressing probe, which then deflects downwards. No surface expansion is observed. The higher the temperature the deeper the temperature gradient, and the more material becomes rubbery. The probe continues to deflect downwards (segment bc) until recrystallization takes place when the probe deflection levels. A noticeable expansion of recrystallized material is detected (segment cd) prior to melting. As the material melts, the probe breaks through the surface and penetrates (segment de). As the temperature is further increased the probe deflects downwards at a slower rate (segment ef). On cooling the probe first is deflected upwards until the melting temperature is reached (segment fg) when recrystallization occurs. The contraction of the material then pulls the probe downwards (segment gh).

Clearly, we have detected a significant difference between bulk and surface properties. This arises from the alignment of the polymer at the surface as it is being extruded. The extra forces on the outside of the extruded material give rise to alignment of the polymer molecules at this surface, and these more highly ordered molecules are able to crystallize more easily.

The sample which underwent a heating and a cooling cycle in the DSC was then analyzed. The free surface exhibits a glass transition, a recrystallization, and a melt during the heating [Fig. 8(a)], whereas the surface in contact with the holding pan undergoes only a clear melting transition [Fig. 8(b)]. These observations can be explained the following way: the surface of the sample has cooled at such a rate during the DSC experiment that the sample reaches its glass transition temperature at the surface before it can fully recrystallize. This is different to the bulk and suggests that the surface cools more quickly than the bulk material.

These results show how micro-thermal analysis may be used to characterize inhomogeneities in properties such as crystallinity and consequently, by supplying spatially re-

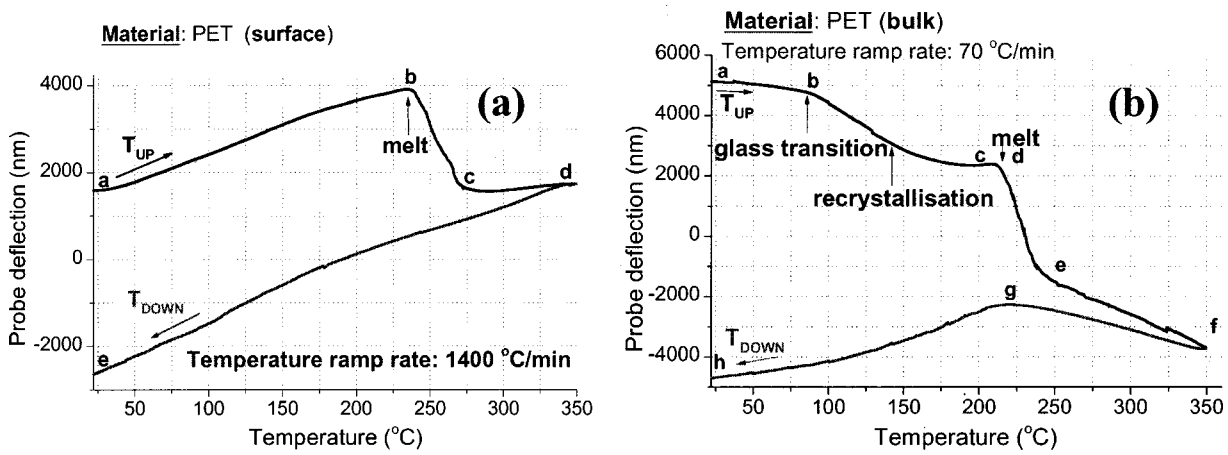

FIG. 7. Localized thermomechanical analysis, using a Wollaston wire probe, (a) of the surface of the quenched PET as supplied; no glass transition is observed indicating that the surface is fully crystalline and (b) of the bulk of the same sample exhibiting a glass transition.

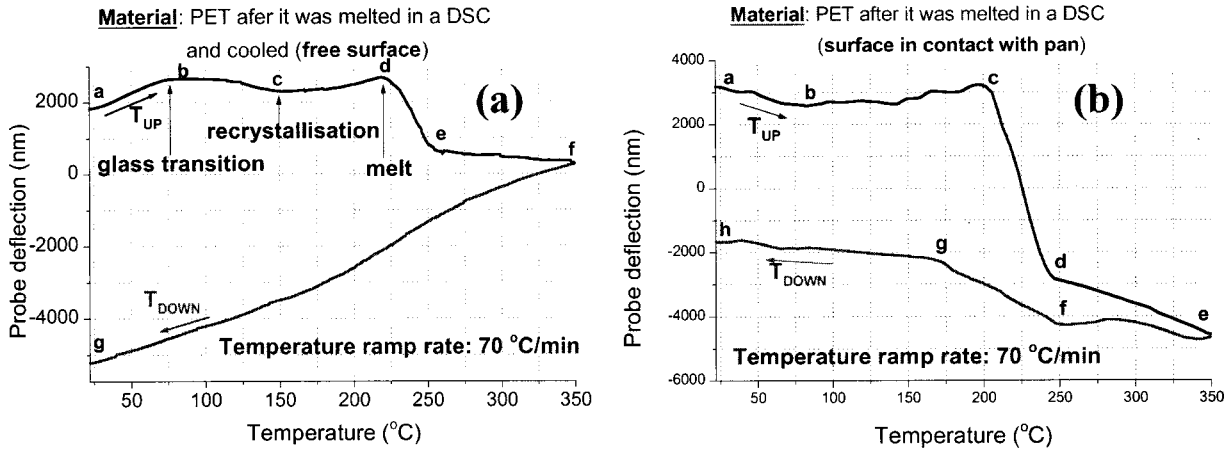

FIG. 8. Localized thermomechanical analysis, using a Wollaston wire probe, (a) of the free surface of the quenched PET after it was melted once; a glass transition is observed indicating that the surface is not fully crystalline and (b) of the surface in contact with the aluminum pan indicating full crystallization.

solved information, can yield a much more complete characterization than is possible with conventional thermal methods.

V. SCANNING THERMAL EXPANSION MICROSCOPY (SThEM) AS A NEW MODE OF THERMAL IMAGING

Varesi and Majumdar[10] have described a method of thermal expansion imaging, termed scanning Joule expansion microscopy, in which Joule heating is applied by means of a modulated electric current passed through an electrically conducting sample. A normal atomic force microscopy probe is used to detect the modulated thermal expansion for purposes of imaging. Our technique differs from this, in that we again use the active thermal probe, either Wollaston or micromachined, to provide localized heating. Its temperature is modulated as it is scanned across the surface of the specimen at a constant underlying force. Local modulated thermal expansion is thus induced, whose amplitude and phase shift (with regard to the heating current) are recorded, using a lock-in amplifier, by monitoring the modulated deflection of the probe, to create images. Appropriate time constants (force feedback and lock-in) and spatial scanning speed were used to minimize artifacts. Three images are recorded simultaneously: topography, amplitude of surface expansion, and phase of surface expansion.

Results obtained imaging the PET/resin sample are presented: Fig. 9 shows images of topography, amplitude, and phase of surface expansion, obtained scanning the same area of sample 1 across the PET/resin boundary, for frequencies ranging from 30 Hz to 10 kHz. The amplitude of the induced probe temperature is estimated at 10 °C. We find that at low frequencies (below about 30 Hz), modulated expansion images recorded using the micromachined probe do not show any discernible contrast between the two areas. The images recorded using the Wollaston probe do show contrast between the PET and the resin, although the boundary between the two areas is not sharp. As the frequency is increased, significant amplitude contrast begins to appear in the micromachined probe images. At 700 Hz, very clear and sharp contrast is observed in the amplitude image taken with the micromachined probe, but not in the phase image. At 2 kHz and above, the contrast in the Wollaston images decreases until, at 10 kHz, sharp contrast is only observed in the amplitude image taken with the micromachined probe. In general, amplitude images give more contrast than phase images, and the amplitude of the surface expansion is larger for the resin than for the PET, indicating a higher coefficient of thermal expansion. This is observed with both types of probe. The measured bulk coefficients of thermal expansion are 63.6 μm/m/ °C and 176.3 μm/m/ °C for the PET and the resin, respectively.

The reason for the apparent better sensitivity of the micromachined probe at higher frequencies, and the ability of the Wollaston wire probe to differentiate between the two regions at lower frequencies, we contend, is largely influenced by two factors: (i) probe/sample contact area and (ii) volume of material heated at a given frequency as determined by the thermal diffusion length. In the case of the Wollaston probe, and at low frequencies, the larger contact area (the probe radius of curvature is 20 μm and the wire diameter is 5 μm), combined with the longer thermal diffusion length, lead to a volume of expanding material whose resulting surface expansion is within the detection limit of the probe. Indeed, sensitivity is determined, to a large extent, by the spring constant: the stiffer the probe, the lower the sensitivity. At higher frequencies, a smaller total volume of heated and thus expanding material results in a reduced modulated surface expansion, which is below the sensitivity of the probe. In the case of the micromachined probe, the contact area between the actual heating element of the probe and the sample is much smaller (the taper is 150 nm wide). However, the silicon pyramid on which the palladium taper is deposited will act as a heat sink. This may act in such a way that heat injected into the sample is reduced and the resulting surface expansion effect diminished. This is more evident at low frequencies where heat diffusion into the pyramid and the rest of the probe is so important that the

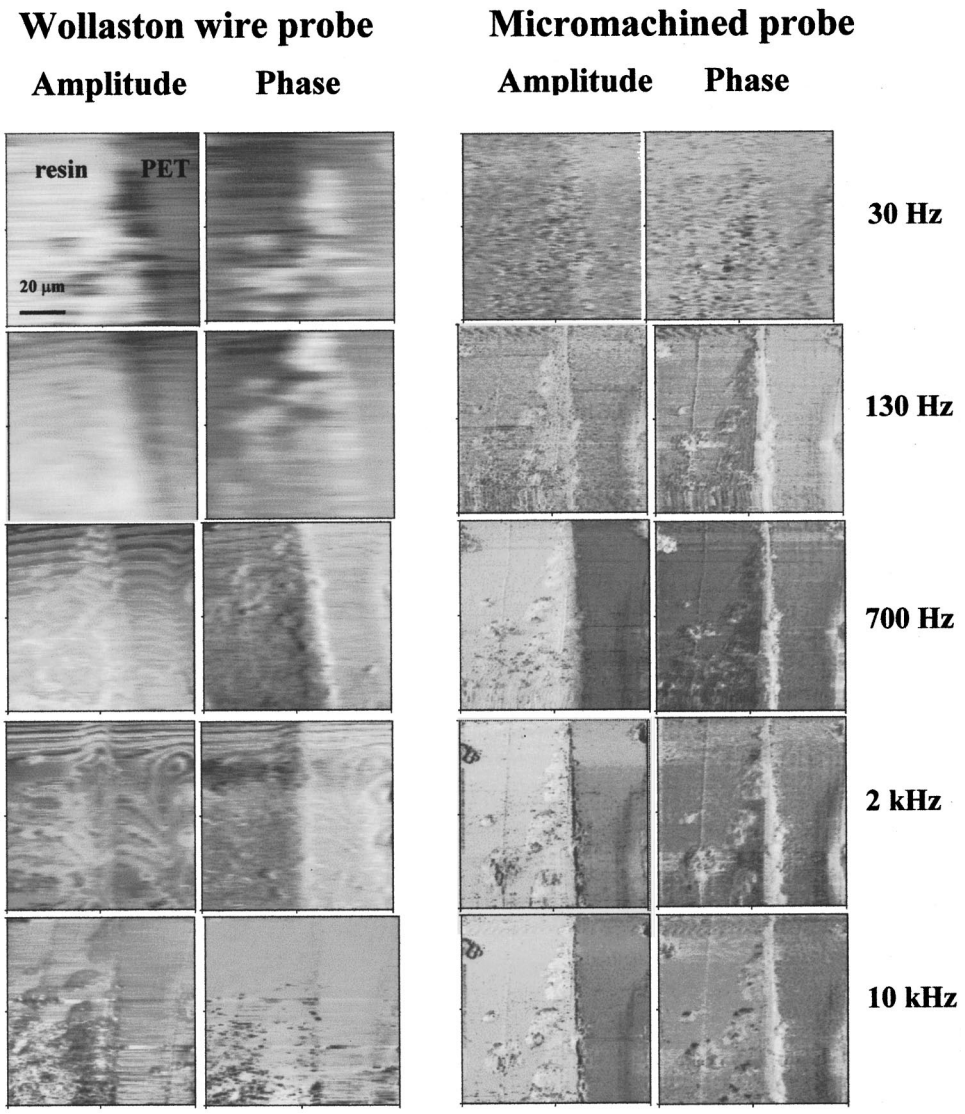

FIG. 9. Thermal expansion images (amplitude and phase) of the polyethylene terephthalate/acrylic resin composite polymeric sample recorded using the Wollaston wire and the micromachined probes. The modulation temperature is 10 °C. The sample is scanned with an underlying constant force.

effect on the sample is not detected and no contrast is observed in the recorded images. However, at higher frequencies, diffusion into the pyramid is reduced. Due to the small spring constant of its cantilever, the probe has a high sensitivity to vertical deflections and is able to resolve the difference in surface expansion between the polymers as observed in our measurements.

Modeling of the behavior of the probes in this mode of operation is being undertaken. It takes into account the thermal and mechanical properties of the probes and the sample, the geometries of the probes, the nature of the heat exchange processes between probe and the sample and the influence of the surrounding environment. This will be the subject of a future publication in which a simple resonance model is also described to account for an observed reversal, in some instances, in image contrast as a function of frequency.

VI. PROGRESS TOWARDS THE DEVELOPMENT OF LOCALIZED PHOTOTHERMAL FTIR SPECTROSCOPY

A number of publications describe versions of scanning probe microscopy (SPM) imaging based on various forms of absorption microscopy and spectroscopy[11] or photothermal effects.[12–14] Oestershultze, Stopka, and Kassing[15] have reviewed the use of SPM techniques for the photothermal characterization of solids and thin films, and near-field Raman spectroscopic imaging has been described by Smith and co-workers.[16,17] Direct absorption of optical power in the near field of an illuminated sample surface has been detected using submicrometer photodiode assemblies consisting of a diode built at the apex of a micromachined pyramidal silicon tip.[18–21] Davis, Williams, and Neuzil[18,19] and Danzebrink, Wilkening, and Ohlesson[20] have used Al–Si Shottky diode probes whose spectral range is similar to that of bulk silicon detectors (from about 400 to 1200 nm, with a maximum absorption at about 950 nm). Dried polystyrene spheres 300 nm wide deposited on glass were resolved in the optical images, and absorption spectra were obtained from individual spheres.[19] Using a total internal reflection setup, structures 250 nm long, 15 nm high, and 60 nm wide were resolved in the optical images.[20] Akamine, Kuwano, and Yamada[21] have used *p-n* junction photodiodes and detected 120 nm sized particles in the optical image in the visible region of the

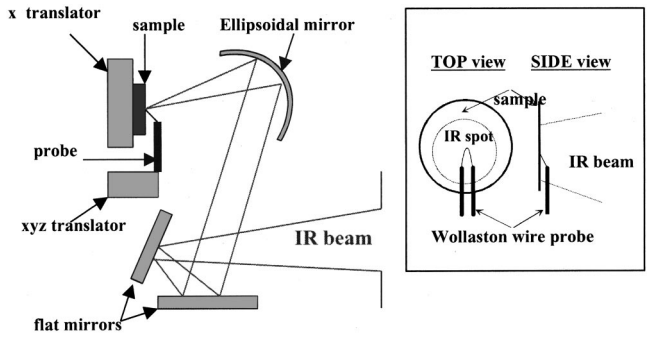

FIG. 10. Schematic diagram of probe and sample arrangement inside the FTIR spectrometer chamber. The inset illustrates the IR illumination of the sample and the probe.

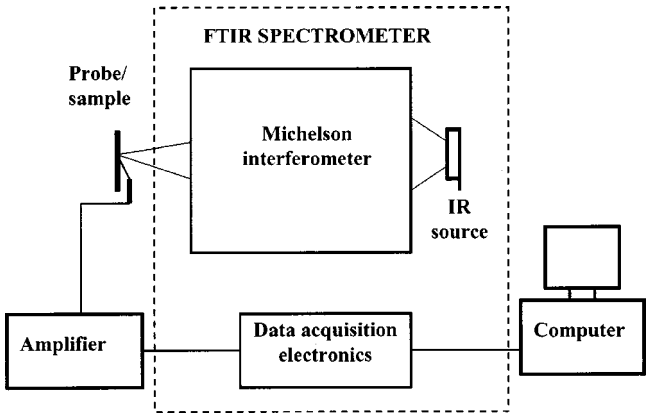

FIG. 11. Schematic of the proximal probe photothermal FTIR spectroscopy measurement system.

spectrum. Recently, Stranick *et al.*[22] have reported an infrared near-field scanning optical microscopy (NSOM) instrument that uses absorption as the contrast mechanism. The system uses near-field probes fabricated from a single mode fluoride glass fiber which supports transmission from 2.2 to 4.5 μm. They have demonstrated a spatial resolution of approximately $\lambda/10$ by recording single wavelength (3.39 μm) IR NSOM images of a TiO_2/melamine nanocomposite. Using a broad band infrared laser source, they have also recorded spectra in the 3 μm range with a signal to noise of approximately 20 in a 1 s dwell time.

Elsewhere[8] we have described the first use of the Wollaston wire resistive probe, operated as a thermometer, to record Fourier transform infrared absorption spectra of specimens by detecting photothermally induced temperature fluctuations at the sample surface. The signal from the probe measures the resulting temperature fluctuations, thus providing an interferogram which replaces the interferogram normally obtained by means of direct detection of the IR radiation transmitted by the sample. As shown in Fig. 10, sample and probe are fitted inside the chamber of a FTIR spectrometer (Vector 22, Bruker UK). Some condensing optics are used to increase the flux at the sample surface in order to increase signal-to-noise ratio. As shown in the inset of Fig. 10, the IR beam is focused on a spot which is 2 mm in diameter. Probe and sample surface are brought into contact at the focal point. The probe is therefore in the path of the beam. Figure 11 shows a schematic diagram of the entire measurement setup. As the sample absorbs the IR radiation, it heats up. The resulting temperature rise of the probe induces changes in its electrical resistance, which are amplified by means of a Wheatstone bridge. The signal from the bridge is fed into the external input of the spectrometer, and the Fourier transform algorithm is performed on this signal after digitization. At present the signal-to-noise ratio is low: however, this particular model of spectrometer has the important feature of being able to perform co-adding without first having to detect the ''center burst'' of the interferogram from an individual scan. Coherent averaging using co-adding is used to pull the useful signal, i.e., the interferogram, out of the noise.

Absorption spectra were obtained for a number of polymers using the Wollaston wire probe to detect the photothermally induced temperature fluctuations. The Michelson interferometer of the spectrometer was run at 2200 Hz (He–Ne fringes count), leading to a frequency content in the interferogram of between 700 and 70 Hz for a wavelength ranging from 2 to 20 μm. The probe can respond to these frequencies without attenuation. We found that the center burst started to show above the noise after approximately 20 co-additions, each of which involved about 1 s of measurement time. After ~1000 co-additions, spectral peaks had become clearly differentiated. The spectra shown here are obtained from two sets of measurements. First, a background measurement is obtained with the probe away from the sample. It represents heating of the probe due to its own absorption of the radiation and heating of the surrounding air. A second measurement is made with the sample in contact with the probe. The two measurements are then subtracted. Absorption spectra obtained using attenuated total reflection (ATR) FTIR spectroscopy are also presented for comparison. An example of both sets of spectra for two particular polymers is shown in Fig. 12. For each material, prominent absorption peaks are clearly resolved.

We have recently performed spectroscopic subsurface detection of a buried polymeric layer. A two layer polymeric system consisting of polyisobutylene (PIB) on top of polystyrene (PS) was spin coated on a glass slide. Samples with varying top layer thickness (from 2 to 15 μm) were produced. The polystyrene layer is of the same thickness (50 μm) for all the samples. The photothermal spectra obtained with the Wollaston probe are shown in Fig. 13. As the thickness of the PIB film increases, the double peak (aromatic) characteriztic of polystyrene at $770-730\,cm^{-1}$ dies away and the PIB C–H stretch at $3000\,cm^{-1}$ stands out increasingly clearly. Detection of the buried PS up to 15 μm thickness of the top PIB layer is thus observed to be possible.

The attainable spatial resolution will depend upon probe size as well as the thermal properties of the sample. Indeed, in the case of a sample with multiple heat sources, the temperature oscillation at a particular point is composed of a contribution due to locally generated heat and superimposed thermal waves from remote sources. Thus, spatial resolution

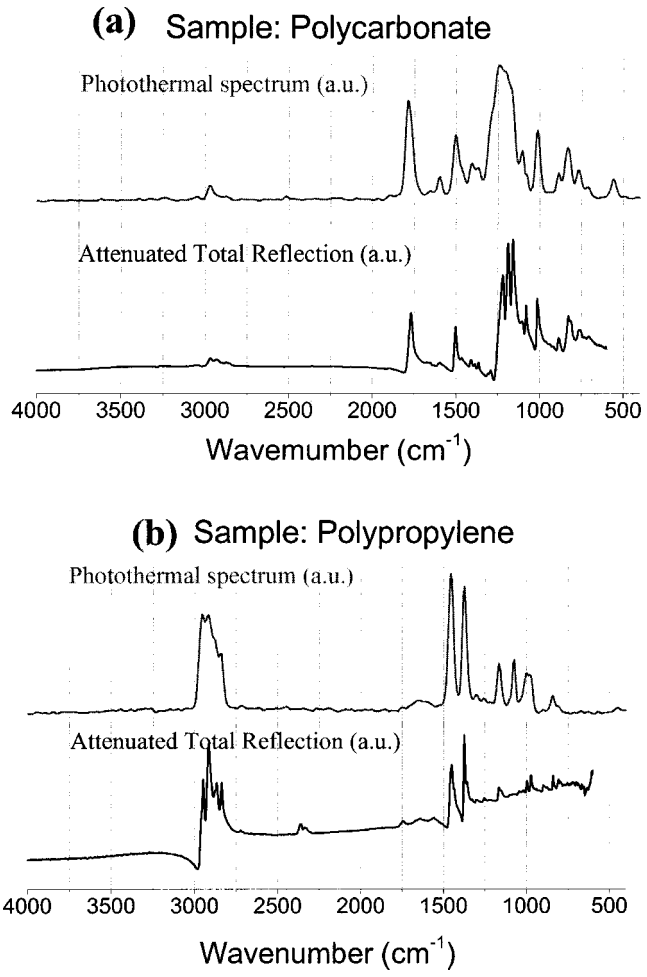

FIG. 12. Examples of spectra obtained using conventional ATR FTIR spectroscopy and proximal probe (Wollaston wire) photothermal FTIR spectroscopy. (a) Polycarbonate and (b) polypropylene. Both sets of spectra are recorded with a wave number resolution of 16 cm^{-1}. The photothermal spectra are the result of 5000 co-additions.

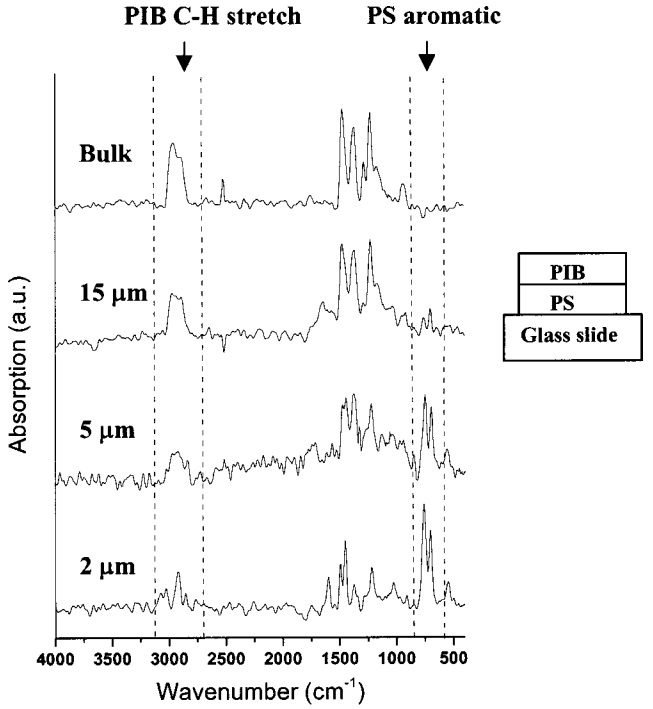

FIG. 13. Photothermal spectra obtained from a bilayer system of polyisobutylene (PIB) on top of polystyrene (PS). The PS layer is 50 μm thick and the PIB layer is 2, 5, and 15 μm thick. The top spectrum was obtained from a bulk sample of PIB. The inset shows the sample structure.

can be affected by thermal wavelength. With a thermoreflectance photothermal microscope that utilizes a HeNe probe laser beam focused to a few microns spot size, Voigt, Hartmann, and Reichling[23] have mapped the Joule effect-induced temperature distribution across a structure of conductive platinum strips (20 μm wide) on a Al_2O_3 substrate. By modulating the excitation current at different frequencies, they have experimentally shown that heat sources such as constrictions are best located at high frequencies, while wave propagation away from these sources can be monitored conveniently at low frequency. This is due to the frequency dependence of the thermal diffusion length. The same considerations apply when our resistive probe, rather than the focused light beam of Voigt and co-workers is used: because in our experiment the light is absorbed across a large area (2 mm wide spot at present), we also have an extended heat source surrounding the detecting probe. Thermal waves generated some distance away from the probe which reach the probe with little attenuation will contribute to the local temperature. In our FTIR system, the electromagnetic radiation at the output of the Michelson interferometer is modulated. The modulation frequencies depend on the wavelength of the radiation as well as the speed of the moving mirror of the interferometer, leading to a range of thermal diffusion lengths (L_t) within the sample. Taking into account the frequency content of the interferogram obtained in a measurement on a typical polymer, L_t ranges from 18 μm at an optical wavelength $\lambda=20$ μm, to 5.5 mm at $\lambda=2$ μm. At first sight the L_t values given above are too large to help in limiting the spread of the temperature profiles to be detected at the submicron level of spatial resolution. However, in principle it would be possible to reduce L_t, either by increasing the speed of the mirror or by introducing a further high-frequency modulation in the tens of kHz range.

We are developing a more powerful source in order to improve signal-to-noise ratio and thus reduce acquisition time. This source consists of a 2-mm-diam hot spot on a refractory target surface, heated by means of the beam from a CO_2 laser. The source is coupled to the input of the Michelson interferometer by means of an infrared optical fiber. IR light at the focal point of the condensing optics is guided to the sample using another IR optical fiber. The sample is located in a scanning probe microscope. Scanning probe photothermal FTIR microscopy/spectroscopy can then be performed. This opens the way to IR microscopy at a spatial resolution well below the diffraction limit of IR radiation, ultimately at a scale of 20–30 nm. In this respect the operating principle differs from that of current FTIR microscopes whose resolution depends on focusing of the infrared light.

VII. CONCLUSIONS

(1) We have demonstrated the versatility of use of cantilevered resistive thermal probes, due to the fact that they can act either as highly localized heat sources or as thermometers. In particular, the combination of SThM with localized thermomechanometry (or localized thermomechanical analysis, L-TMA) shows promise.

(2) For samples of quenched PET, we have compared data obtained by L-TMA and by conventional bulk thermal analysis (in this case differential scanning calorimetry or DSC). Inhomogenieties within materials that cannot be detected using conventional bulk thermal methods are revealed by L-TMA. The resultant spatially resolved information can yield a much more complete characterization than is possible with conventional thermal methods.

(3) Scanning thermal expansion microscopy provides a new mode of thermal imaging. Strong image contrast is determined by differences in thermal expansivity, although thermal conductivity variations may also introduce complications.

(4) We have outlined progress towards the development of localized Fourier transform infrared spectroscopy (FTIR): here the probe, in this case operated in the temperature sensing mode, detects the photothermal response of a specimen exposed to the beam and heated thereby. The spatial resolution will be determined by the probe size rather than the IR wavelength, provided that the probe size is small compared to the characteriztic distances describing the spatial variations in temperature that are to be detected. These variations can arise from the spatial variations in absorbance as discussed elsewhere.[8] Further improvement in spatial resolution can be made possible by making use of the damped nature of thermal waves such that the thermal diffusion length is smaller than the probe size. Probe size then determines resolution, and infrared spectroscopy/microscopy at a spatial resolution better than the diffraction limit can be achieved. For polymer samples, prominent absorption peaks were clearly resolved, corresponding satisfactorily with peaks obtained by conventional ATR-FTIR. Spectroscopic detection of buried polymeric layers was also achieved.

ACKNOWLEDGMENTS

This work was made possible by funding from the U.K. Engineering and Physical Sciences Research Council. The authors also thank T A Instruments Inc. for financial support and Bruker UK for the loan of equipment.

[1]D. M. Price, M. Reading, A. Hammiche, and H. M. Pollock, Int. J. Pharm. **192**, 85 (1999).
[2]A. Hammiche, M. Reading, H. M. Pollock, M. Song, and D. J. Hourston, Rev. Sci. Instrum. **67**, 4268 (1996).
[3]A. Hammiche, H. M. Pollock, M. Song, and D. J. Hourston, Meas. Sci. Technol. **7**, 142 (1996).
[4]A. Hammiche, H. M. Pollock, M. Song, D. J. Hourston, and M. Reading, J. Vac. Sci. Technol. B **14**, 1486 (1996).
[5]H. M. Pollock, A. Hammiche, M. Song, D. J. Hourston, and M. Reading, J. Adhes. **67**, 217 (1998).
[6]D. M. Price, M. Reading, A. Caswell, A. Hammiche, and H. M. Pollock, Microsc. Anal. **65**, 17 (1998).
[7]D. M. Price, M. Reading, A. Hammiche, H. M. Pollock, and M. G. Branch, Thermochim. Acta **332**, 143 (1999).
[8]A. Hammiche, H. M. Pollock, M. Reading, M. Claybourn, P. Turner, and K. Jewkes, Appl. Spectrosc. **53**, 810 (1999).
[9]H. Zhou, A. Midha, G. Mills, S. Thoms, S. K. Murad, and J. M. R. Weaver, J. Vac. Sci. Technol. B **16**, 54 (1998).
[10]A. Majumdar and J. Varesi, J. Heat Transfer **120**, 297 (1998).
[11]J. M. R. Weaver, L. M. Walpita, and H. K. Wickramasinghe, Nature (London) **342**, 783 (1989).
[12]C. C. Williams and H. K. Wickramasinghe, SPIE Vol. 897, Scanning Microscopy Technologies and Application, 1988, p. 129.
[13]S. Grafstrom, J. Kowalski, R. Neumann, O. Probst, and M. Wortge, J. Vac. Sci. Technol. B **9-2**, 568 (1991).
[14]N. Trannoy, P. Grossel, and M. Troyon, Probe Microsc. **1**, 201 (1998).
[15]E. Oestershultze, M. Stopka, and R. Kassing, Microelectron. Eng. **24**, 107 (1994).
[16]D. A. Smith, S. Webster, M. Ayad, S. D. Evans, D. Fogherty, and D. N. Batchelder, Ultramicroscopy **61**, 247 (1995).
[17]S. Webster, D. N. Batchelder, and D. A. Smith, Appl. Phys. Lett. **72**, 1478 (1998).
[18]R. C. Davis, C. C. Williams, and P. Neuzil, Appl. Phys. Lett. **66**, 2309 (1995).
[19]R. C. Davies and C. C. Williams, Appl. Phys. Lett. **69**, 1179 (1996).
[20]H. U. Danzebrink, G. Wilkening, and O. Ohlesson, Appl. Phys. Lett. **67**, 1981 (1995).
[21]S. Akamine, H. Kuwano, and H. Yamada, Appl. Phys. Lett. **68**, 579 (1996).
[22]S. J. Stranick, R. R. Cavanagh, D. B. Chase, C. E. Jordan, C. A. Michaels, and L. J. Richter, presented at the 10th International Conference on Scanning Tunneling Microscopy/Spectroscopy and Related Proximal Probe Microscopy, 19–23 July 1999, Seoul, Korea.
[23]P. Voigt, L. Hartmann, and M. Reichling, J. Appl. Phys. **80**, 2013 (1996).